ISBN: 978-3-95450-231-8 ISSN: 2673-5490 doi: 10.18429/JACoW-IPAC2023-THPM125

HIGH EFFICIENCY, 1 MW, 1 MeV ACCELERATOR FOR ENVIRONMENTAL APPLICATONS*

M. Shumail†, G. Bowden, V. Dolgashev SLAC National Accelerator Laboratory, Menlo Park, USA
D. Packard, General Atomics, San Diego, USA
P. Borchard, Dymenso LLC, San Francisco, USA

Abstract

We present design of a normal conducting, high efficiency linac that would provide a CW beam of 1 MW electrons at 1 MeV energy for various environmental applications. When a flowing sheet of wastewater is exposed to such a beam, various radiation-induced reactants are generated that lead to water purification by decomposing the chemical and biological pollutants therein. Such a linac could treat about 20 million gallons of wastewater per day with an ample dose of 1 kGy. Our linac comprises of three optimized accelerating rf cavities operating at 476 MHz. A compact rf distribution manifold splits the rf power from a 1-MW klystron in the appropriate ratio and phase for each accelerating cavity. The beam capture efficiency is 82% and the rf-to-beam efficiency is 94.5%. The total length of our accelerator is 2 m, which includes the 30 keV gun, the buncher cavity, and the accelerating cavities. In this paper, we present the corresponding beam dynamics, the implementation of rf couplers and feeding manifold, and the steady-state thermal analysis.

INTRODUCTION

Various studies and pilot scale projects around the world have shown the efficacy of electron beam radiation treatment of municipal and industrial wastewater [1-4]. In this process, the detoxification of contaminated water is achieved by the reaction of biological and chemical pollutants with highly reactive species: hydrated electron, OH free radical and H atom, that are generated because of electron beam induced radiolysis of water [5, 6]. The industrial scale adoption of electron beam induced radiation treatment of wastewater requires a reevaluation of the current state of the art industrial class of accelerators. It also requires application of modern approaches and technologies to improve linac efficiency at high average power and reduce the overall cost. Systems with high wall-to-beam efficiency are of paramount importance as they have potential to reduce the cost of operation and alleviate the complexities associated with the heat management of linac. Special consideration should also be given to minimize the capital cost. Recently, we have explored various theoretical methodologies and designs for high average power and high efficiency normal conducting linacs for industrial applications [7-9].

* Work supported by USA DOE through Accelerator Stewardship program under FWP 100624.
† shumail@slac.stanford.edu

LINAC DESIGN

Here, we present the physics design of a 2-meter long, 476 MHz, 1 MW, 1 MeV linac. The conceptual layout is shown in Fig. 1 (a).

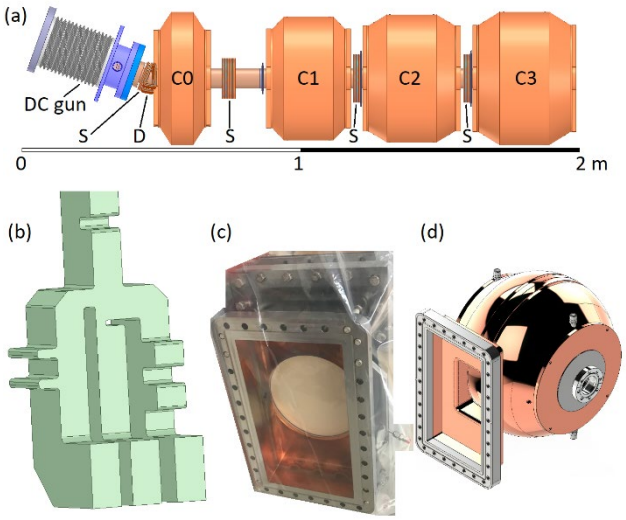

Figure 1: (a) Layout of the linac showing the DC gun, dipole magnet (D), solenoids (S), buncher cavity (C0), and the three accelerating cavities (C1, C2, C3). (b) RF power distribution manifold vacuum space. (c) One of three vacuum windows. (d) Solid model of cavity C3.

The linac comprises of a buncher cavity and four accelerating cavities with optimized shunt impedance. This design is based on an economical low voltage thermionic DC gun [10] already available to us and employs a dipole and four solenoid magnets to steer the beam. The gun injects a CW electron beam of 30 keV, 1.225 A and the output of the linac is a bunched beam of 955 keV, 1.02 A. The output electron beam window was outside the scope of this study.

The rf-to-beam efficiency of the accelerator is 94.5%. The rf power lost in the copper walls is 36 kW and beam power loss is 18 kW. The mean$\pm$rms energy spread of top ninety percentile of the bunch at the output is 997$\pm$43 keV. The total rf power input to any cavity doesn't exceed 500 kW. The rf power is supplied through WR2100 waveguide by a CW, 476 MHz, 1 MW klystron [11] which is available at SLAC. The linac will be housed in a nearby shielded room and fed with rf power through a single WR2100 waveguide. This shielded room has 2-feet-thick concrete walls and a 6-inch-thick steel door. It will be equipped with Personal Protection System at the time of linac commissioning. Inside the shielded room, the WR2100 rf feed will be divided into three feeds for the accelerating cavities.

ISBN: 978-3-95450-231-8 ISSN: 2673-5490 doi: 10.18429/JACoW-IPAC2023-THPM125

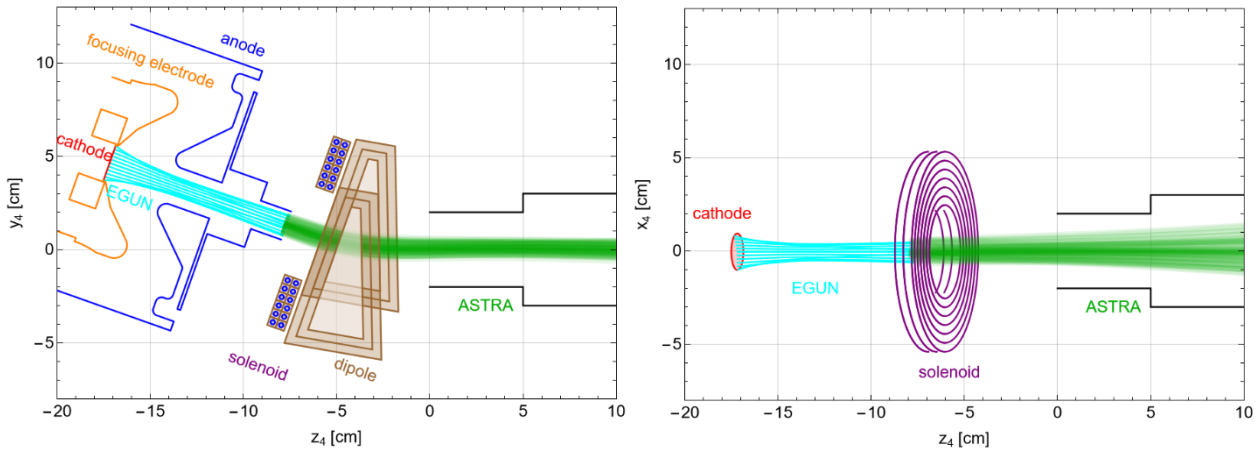

Figure 2: Simulation results of the 30 kV DC gun with a solenoid and a dipole magnet. The blue lines indicate reference trajectories obtained from EGUN simulation while the green lines show reference trajectories as obtained from ASTRA simulation. Here, z_4 is the coordinate along the linac axis. Note that the dipole plane is also rotated.

Figure 1 (b) shows the design of the rf power distribution network that divides the klystron power with appropriate magnitude and phase for the three accelerating cavities (see the first two rows of Table 1). The distribution network design includes chokes for matching and phase adjustments. In future, we will replace these chokes with cylindrical posts.

To isolate the vacuum of the cavities from the gas-filled waveguides, we will employ three vacuum rf windows that were used for PEP-II cavities [12, 13]. One such window is shown in Fig. 1 (c) where the cavity side 16″ × 9″ inch flange is visible while the WR2100 flange is on the back side. These windows are rated for 500 kW, CW rf power and can be safely used for all the accelerator cavities in our design. Figure 1 (d) shows CAD model of the last of the three accelerating cavities with 16″ × 9″ vacuum flange. The buncher cavity will have coaxial coupler and would be separately fed by a 500-watt solid state CW amplifier.

DC Gun Simulation

The beam simulation results of this gun are shown in Fig. 2. The gun axis is tilted at an angle of about 20° with respect to the linac axis. This arrangement is done to protect the cathode from the back scattered electrons. This gun is to be operated in space-charge limited regime with a 3-cm^2 cathode and without any grid.

First, we used Ansys Maxwell [14] to obtain the 3D magnetic fields from the solenoid and dipole. Then we ran 2D electrostatic simulation using EGUN [15] with cathode at 1400 K to obtain the particle trajectories shown in blue in Fig. 2. For this 2D analysis we ignored the field of the dipole magnet as those are negligible in the relevant region. The EGUN simulation also showed that this gun could provide a CW electron beam of 1.225 A at 30 keV.

Obtaining the particle distribution from the previous analysis, we performed the 3D beam dynamics simulation using ASTRA [16, 17] with the magnetic fields of both the solenoid and the dipole. This generated the trajectories that are shown in green in Fig. 2. From these trajectories, we obtain the linac axis as the one on which the mean transverse position and momentum of the particles is zero.

Buncher and Accelerating Cavities Simulation

Figure 3 (a) shows a longitudinal-half cross section of the linac without the rf couplers. The buncher cavity, and the accelerator cavities were optimized in Ansys HFSS [18] to maximize shunt impedance assuming the estimated beam energy range as given in Table 1. The amplitude of the longitudinal rf electric field inside the cavities and the static magnetic field of the solenoids are shown in Fig. 3 (b). The phases of the beam-loaded rf fields in the cavities, as used in ASTRA, are also shown. A snapshot of steady-state particle distribution obtained through this simulation is shown as particle energy (E) versus longitudinal position (z) in Fig. 3 (c). The particles are color-coded according to the rf-cycle during which they got injected from the gun. About 82% of the particles, which constitute 1.02 A current, get captured and accelerated out of the linac at mean energy of 0.955 MeV.

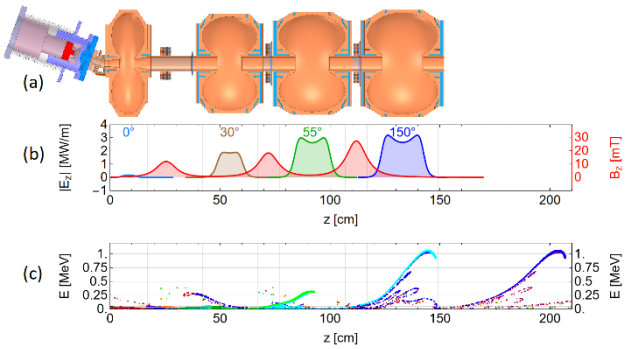

Figure 3: (a) Cross section of the linac. (b) Longitudinal rf electric and DC magnetic field amplitudes along the axis. (c) A snapshot of energy distribution of the particles at steady-state along the linac.

The transverse and longitudinal phase space plots of the electron beam at the output of the linac are shown in Fig. 4. Note that the linac beam pipe radius is 3 cm. The mean±rms energy spread for all the particles at the output is 955±168 keV. The corresponding rms longitudinal spread is 6 cm while the rf wavelength is 63 cm.

ISBN: 978-3-95450-231-8 ISSN: 2673-5490 doi: 10.18429/JACoW-IPAC2023-THPM125

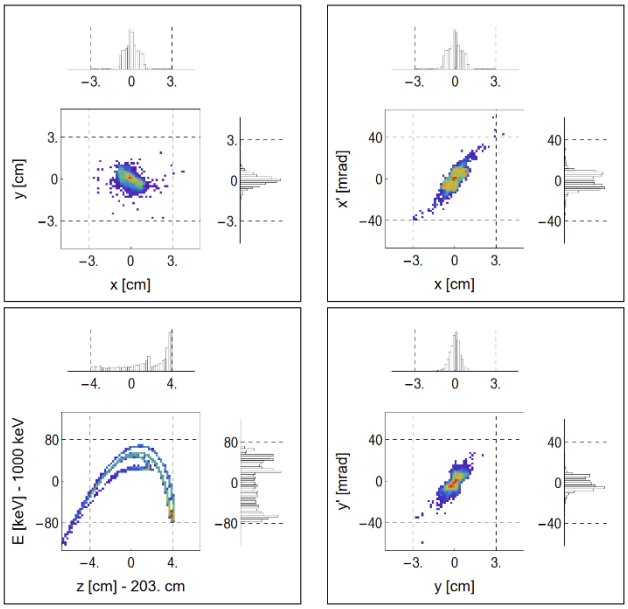

Figure 4: The transverse and longitudinal phase space plots of the electron beam at the output of the linac (z = 203 cm).

Beam Loading Analysis

We performed detailed beam loading analysis using the results obtained from ASTRA beam dynamics simulations to calculate beam-induced field and generator-induced field for each cavity. These were then used to obtain the required rf generator phase (ϕ_g) and power (P_g), power gained by the beam (P_b), power lost in the cavity walls (P_c), and the required coupling coefficients (β) for the cavities. Table 1 summarizes these results along with quality factor (Q_0) and shunt impedance (r_s) of the cavities. In the last row of Table 1 we list the energy (E) ranges of the particles inside each cavity that we used to calculate r_s. Given the values of the coupling coefficients (β), we have designed a loop coupler (not shown) for the buncher cavity and 16" × 9" waveguide couplers for the accelerating cavities like the one shown in Fig. 1 (d).

Table 1: Cavity Parameters

Quantities	C0	C1	C2	C3
ϕ_g (°)	2	18	57	152
P_g (kW)	0.43	171	370	450
P_b (kW)	0.41	167	356	432
P_c (kW)	0.02	4	14	18
β	22	39.3	26.6	25.1
Q_0	30,420	35,170	38,500	41,890
r_s (MΩ)	4.3	7.8	11.2	12.5
E (keV)	30	30 – 200	200 – 600	600 – 1000

Thermal Analysis

The DC power requirement of the dipole and solenoid magnets is in the range of 10 – 80 W. These magnets will be built using square, hollow, copper tubes that would carry low conductivity water for cooling.

For the cavities, besides the rf wall losses mentioned in Table 1, we also calculated the power lost by beam hitting the cavity walls. The total wall loss density due to both rf and beam is shown in Fig. 5 (a). For the buncher cavity, we implemented two azimuthal cooling channels of cross section 5 mm × 20 mm that can be seen as tiny rectangles in Fig. 5 (b). We assume 30°C water flowing into each of these channels at a rate of 4 gallons per minute (gpm). For the accelerating cavities, we implemented similar cooling channels but of cross section 5 mm × 10 mm with 30°C water flowing into each channel at a rate of 2 gpm. The fluid dynamic estimates give a convective heat coefficient of 12 kW/m^2/K for both cases. The thermal simulations were performed using Ansys Workbench [19] and the resultant steady-state temperature distribution is shown in Fig. 5 (b).

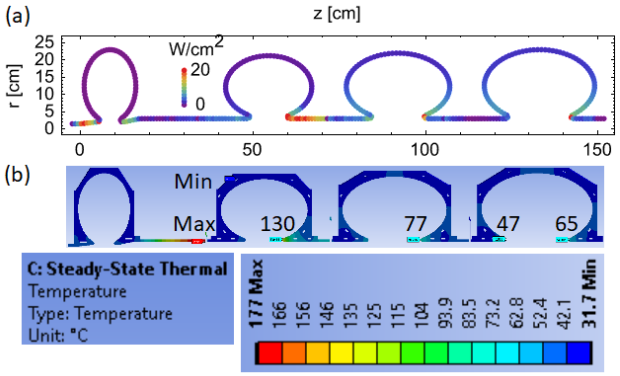

Figure 5: (a) Total (rf and beam) wall loss density on the accelerator surface. (b) Steady-state temperature distribution with convective heat transfer coefficient of 12 kW/m^2/K along the cooling pipe surfaces.

CONCLUSION

We have presented the physics design for a 1 MW, 1 MeV electron linac with rf-to-beam efficiency of 94%. This includes a summary of the detailed beam dynamics studies. The beam loading analysis is done to calculate rf power and phase requirements for each cavity and their coupling coefficients. The cavity couplers and the rf distribution network is designed accordingly. A steady-state thermal analysis is also presented.

Currently we are performing the particle-in-cell simulations to confirm the beam loading calculations. We are also fabricating the last accelerating cavity (C3) and are planning to test it at high power with the klystron as a demonstrator for the full linac.

REFERENCES

[1] B. Han, J. K. Kim, Y. Kim, J. S. Choi, K. Y. Jeong, "Operation of industrial-scale electron beam wastewater treatment plant," *Radiat. Phys. Chem.*, vol. 81, pp. 1475-1478, 2012. doi:10.1016/j.radphyschem.2012.01.030.

[2] M. H. O. Sampa *et al.*, "Remediation of polluted waters and wastewater by radiation processing," *Nukleonika*, vol. 52, pp. 137–144. 2007.

ISBN: 978-3-95450-231-8 ISSN: 2673-5490 doi: 10.18429/JACoW-IPAC2023-THPM125

[3] Takasz, E., "High energy radiation treatment of textile dye containing water," Report from a Coordinated Research Project Meeting, IAEA, Vienna. 2004.

[4] D. Solpan, O. Gueven, "Decolouration and degradation of some textile dyes by gamma irradiation," *Radiat. Phys. Chem.*, vol. 64, pp. 549–558, 2002.

[5] G. V. Buxton, C. L. Greenstock, W. P. Helman, and A. B. Ross, "Critical review of rate constants for reactions of hydrated electrons, hydrogen atoms and hydroxyl radicals (·OH/·O$^-$) in aqueous solutions," *J. Phys. Chem. Ref. Data*, vol. 17, pp. 513 – 886, 1988. doi:10.1063/1.555805

[6] R. O. Abdel Rahman and Y.-T. Hung, "Application of ionizing radiation in wastewater treatment: an overview," *Water*, vol. 12, no. 1: 19, 2020. doi:10.3390/w12010019

[7] V. Dolgashev and S. Tantawi, "Design of high efficiency high power electron accelerator systems based on normal conducting rf technology for energy and environmental applications", submitted to the Office of High Energy Physics, SLAC, Menlo Park, USA, Apr. 2018. doi:10.2172/1441166

[8] M. Shumail and V. A. Dolgashev, "Efficiency analysis of high average power linacs," in *Proc. 9th International Particle Accelerator Conf. (IPAC'18)*, Vancouver, BC, Canada, Apr.-May 2018, pp. 4970-4973. doi:10.18429/JACoW-IPAC2018-THPML125

[9] M. Shumail, V. A. Dolgashev, and C. Markusen, "Design of high efficiency high power CW linacs for environmental and industrial applications," in *Proc. 9th International Particle Accelerator Conf. (IPAC'18)*, Vancouver, BC, Canada, Apr.-May 2018, pp. 4974-4976. doi:10.18429/JACoW-IPAC2018-THPML126

[10] R. F. Koontz, "CID Thermionic Gun System," in *Proc. 1981 Linear Accelerator Conf. (LINAC'81)*, Santa Fe, New Mexico, USA, Oct. 1981, pp. 62-64.

[11] E. Jongewaard *et al.*, "Operating results for the PEP II 1.2 MW klystron," in *Proc. 5th European Particle Accelerator Conf. (EPAC'96)*, Barcelona, Spain, Jun. 1996, p. 2155.

[12] M. Neubauer *et al.*, "High-power RF window design for the PEP-II B Factory," in *Proc. 4th European Particle Accelerator Conf. (EPAC'94)*, London, England, Jun.-Jul. 1994, pp. 2033-2035.

[13] M. Neubauer *et al.*, "High-power testing of PEP-II RF cavity windows," in *Proc. 5th European Particle Accelerator Conf. (EPAC'96)*, Barcelona, Spain, Jun. 1996, p. 2059.

[14] Ansys Maxwell, https://www.ansys.com/products/electronics/ansys-maxwell

[15] W. B. Herrmannsfeldt, "EGUN: An electron optics and gun design program," SLAC, Menlo Park, USA, Rep. SLAC-331, 1988. doi:10.2172/6711732.

[16] K. Flottmänn, S. M. Lidia, and P. Piot, "Recent improvements to the ASTRA particle tracking code", in *Proc. 20th Particle Accelerator Conf. (PAC'03)*, Portland, OR, USA, May 2003, pp. 3500-3502.

[17] A Space Charge Tracking Algorithm, https://www.desy.de/~mpyflo/

[18] Ansys HFSS, https://www.ansys.com/products/electronics/ansys-hfss

[19] Ansys Workbench, https://www.ansys.com/products/ansys-workbench